Influence of the Caribbean Sea eddy field on Loop Current predictions

Matthieu Le Hénaff[1,2]*, Vassiliki H. Kourafalou[3],
Yannis Androulidakis[3,4], Nektaria Ntaganou[3,5]
and HeeSook Kang[1,2]

[1]Cooperative Institute for Marine and Atmospheric Studies (CIMAS), University of Miami, Miami,
FL, United States, [2]National Oceanic and Atmospheric Administration (NOAA) Atlantic Oceanographic
and Meteorological Laboratory (AOML), Miami, FL, United States, [3]Rosenstiel School, University of
Miami, Miami, FL, United States, [4]Department of Civil Engineering, Laboratory of Maritime Engineering
and Maritime Works, Aristotle University of Thessaloniki, Thessaloniki, Greece, [5]Center for Ocean-
Atmospheric Prediction Studies (COAPS), Florida State University, Tallahassee, FL, United States

Previous studies have shown how the passage of eddies from the Caribbean Sea
(CS) to the Gulf of Mexico (GoM) can impact the Loop Current (LC) system, in
particular the detachments of LC Eddies (LCEs). Here we used numerical
modeling to investigate the impact of the eddy field in the CS on LC
predictions. We used a HYCOM ocean model configuration of the North
Atlantic at 1/12° resolution to perform two data-assimilative experiments: one
in which all available observations were assimilated (*Ref*), and one in which all
available observations were assimilated except in the CS, where climatological
altimetry values were assimilated instead of actual observations, leading to
dampening the mesoscale activity there (*NoCarib*). These experiments took
place in 2015, when the LC was very active with several LCE detachments, re-
attachments, and separations. Each of these experiments was used to initialize 28
60-day forecast simulations every 10 days. In terms of model Sea Surface Height
(SSH), the forecasts initialized with the *Ref* experiment had, on average, lower
errors than the forecasts initialized with the *NoCarib* experiment in the
southeastern part of the GoM, with a peak during the 31-40 day forecast
period. More importantly, the errors in predicting the date of the next LCE
detachment or separation were smaller in the forecasts initialized from the more
realistic *Ref* experiment. Finally, the forecasts initialized by the *NoCarib*
experiment showed a much higher level of false negatives predictions,
meaning that no LCE detachment was predicted whereas a detachment
actually happened. Overall, 68% of LCE detachments were predicted with an
error smaller than 15 days in the forecasts initialized from the more realistic *Ref*
experiment, but only 32% in the forecasts initialized from the *NoCarib*
experiment, stressing the importance of the CS eddy field for predicting the LC
evolution. These findings have implications on the GoM predictability,
highlighting the need to either run data-assimilative models covering both the
GoM and the CS, or pay particular attention to accurate boundary conditions for
limited-area GoM models.

1 Introduction

The Loop Current (LC) is the main dynamical feature in the Gulf of Mexico (GoM). Characterizing and predicting the state of the LC has important implications, as it affects all ranges of ocean-related processes in the GoM, from larval connectivity to pollution transport or oil platform operations (e.g. Lara-Hernández et al., 2019; Le Hénaff et al., 2012a; Kaiser and Pulsipher, 2007). This led the National Academy of Sciences, Engineering, and Medicine to implement the Understanding Gulf Ocean Systems (UGOS) initiative as part of its Gulf Research Program, to support research related to ocean observations and modeling in the GoM to improve the understanding and forecasting of the LC dynamics. This study focuses on the forecasting aspect, using numerical methods to examine the influence of the Caribbean Sea eddy field.

The LC is a component of the North Atlantic western boundary current, upstream of the Gulf Stream. It enters the GoM in the south, through the Yucatan Channel between the Yucatan Peninsula in Mexico and the western tip of Cuba, and it exits the GoM to the east, through the Straits of Florida between Florida, in the US, and the northern coast of Cuba. Inside the GoM, the shape of the LC evolves in a peculiar way, from a retracted, or port-to-port, position in which the LC flows almost directly from the Yucatan Channel to the Straits of Florida, to an extended position in which the LC reaches the edge of the northeastern GoM continental shelf, before turning anticyclonically toward the GoM exit in the southeast of the basin.

When it is fully extended, the LC sheds an anticyclonic eddy called a Loop Current Eddy (LCE). LCEs are large eddies, with a diameter of 300 to 400 km at separation, and it takes about 8 months for LCEs to reach the western boundary of the GoM, at which stage their initial diameter decreased by 55% (Vukovich, 2007). Eventually, LCEs break apart after colliding with the continental shelf of the western GoM, or through the interactions with local mesoscale eddies (Vidal et al., 1992; Lipphardt et al., 2008). The shedding of an LCE leads to the sudden southward shift of the LC to its retracted position. The LC can experience several temporary detachments and reattachments of an LCE before the final separation (Schmitz, 2005; Le Hénaff et al., 2012b; Le Hénaff et al., 2014). The period between two LCE separations, called the LC separation period, varies from a few weeks to 18 months, with the dominant modes at 6, 9 and 11 months, and a mean value close to 9 months (Leben, 2005; Dukhovskoy et al., 2015).

The physical mechanisms inside the GoM that explain the behavior of the LC have been the topics of many studies. A reference analytical study was performed by Pichevin and Nof (1997), who characterized the LC as a low-density water mass entering a basin of higher density, the GoM, from the south, which is forced to turn east under the Coriolis force. The authors demonstrate that there is no steady state possible for such a flow, which they identify as the imbalance paradox, and that, as a result, the current must shed eddies that will then drift westward under the beta effect. Using a comparable analytical framework, Lugo-Fernández (2018) found that the LC intrusion is due to an initial transport imbalance at the entrance of the GoM that creates a volume storage inside the LC. This storage in turns creates a sea-level difference across the LC that reinforces the northward flow

into the LC (Lugo-Fernández, 2018). In parallel with these analytical studies, model studies have suggested that the LCE shedding process involves mixed barotropic and baroclinic instabilities (Hurlburt and Thompson, 1980; Hurlburt and Thompson, 1982; Chérubin et al., 2006). Recently, observations confirmed that baroclinic instabilities contribute to the meandering of the LC and intensify during the LCE shedding process (Donohue et al., 2016a; Donohue et al., 2016b). The meandering of the LC is closely associated with the presence of cyclonic frontal eddies along its edge. These frontal eddies are usually observed to be more developed on the eastern flank of the LC, where they often contribute to the necking-down of the LC and to the initial detachment of an LCE (Schmitz, 2005; Le Hénaff et al., 2014; Hiron et al., 2020). Frontal eddies are also observed on the western side of the LC, where they are also found to contribute to the LCE shedding (Zavala-Hidalgo et al., 2003).

At the entrance of the GoM, in the Yucatan Channel, the total transport incoming into the GoM was found to be 27.6 Sv on average, based on mooring observations (Candela et al., 2019). Mooring observations also suggested that periods of cumulative anticyclonic vorticity fluxes are associated with phases of extension of the LC, whereas periods of cumulative cyclonic vorticity fluxes are associated with the retraction of the LC, which sometimes coincide with the shedding of an LCE (Candela et al., 2002). On the other hand, using numerical modeling and observations, Oey (2004) suggested that cyclonic vorticity flux anomalies coming through the Yucatan Channel are associated with the extension of the LC, whereas anticyclonic vorticity flux anomalies are associated with the triggering of the LC retraction or LCE shedding. Oey (2004) also stressed that further research is necessary to better assess these mechanisms.

Compared to the GoM interior and the Yucatan Channel that have been extensively investigated, and although directly upstream of the LC, the Caribbean Sea (CS) has received little attention in the LC problem. Oey et al. (2003), using modeling, found that the variations in the wind-induced transport into the CS tend to shorten the LC shedding interval in the GoM, whereas the presence of anticyclonic eddies in the CS tend to increase it. Similarly, Garcia-Jove et al. (2016) found that suppressing eddies in the CS in their ocean model tends to reduce the number of LCE separations. Using observations, Athié et al. (2012) found that cyclonic eddies present in the CS and entering the GoM on the western side of the incoming LC are often involved in the LCE separation process. Chang and Oey (2012) found that the seasonal variations in wind patterns in the CS, with strong trade winds in summer and winter, favor the shedding of LCEs during those seasons. Androulidakis et al. (2021) found, using observations and numerical models, that the passage of anticyclonic eddies from the CS to the GoM in the Yucatan Channel is more common during retracted LC phases, and that such passages tend to precede, by 5 to 10 days, an eastward shift of the LC in the Yucatan Channel and a retraction of the LC in the GoM. This agrees with Sheinbaum et al. (2016) who, using mooring observations, found that eastward shifts of the main current in the Yucatan Channel appear to be associated with vorticity perturbations coming from the CS and tended to precede eddy detachments.

However, they stressed that the significance of these vorticity perturbations on the shedding process remain to be determined.

In this study, we aim to quantify to what extent the eddy activity in the CS influences the LC shedding process inside the GoM and its prediction. To do so, we implemented numerical experiments that consist of two series of ocean forecasts, one with realistic initial conditions, and one in which the mesoscale eddy activity in the CS has been dampened. The experiments took place in 2015, a year when the LC was very active with several LCE detachments, re-attachments, and separations. Following this introduction (Section 1), Section 2 presents the model and the experimental set-up, Section 3 describes our results, and Section 4 provides a discussion and the conclusions.

2 Methods

2.1 Model

For our numerical experiments, we used the Hybrid Coordinate Ocean Model (HYCOM, Bleck, 2002; Chassignet et al., 2003; Halliwell, 2004). The model was implemented over the North Atlantic (Figure 1). This model configuration is similar to the Observing System Simulated Experiment (OSSE) system forecast model described in detail in Halliwell et al. (2017a). In particular, the model grid has a 1/12° (0.08°) horizontal resolution and 26 hybrid vertical levels, which is comparable to most global operational ocean systems. One difference with Halliwell et al. (2017a) is that the model is forced at the surface by the NAVy Global Environmental Model (NAVGEM) that replaced the Navy Operational Global Atmospheric Prediction System (NOGAPS). Similar to the configuration introduced by Halliwell et al. (2017a), the model is implemented with a data assimilation filter that is based on a statistical interpolation scheme. The details of the data assimilation filter are described by Halliwell et al. (2014). The forecast error covariance statistics necessary for the data assimilation step are estimated using a multi-year free running simulation of the same model. This model configuration has been fully evaluated by Halliwell et al. (2017a) and implemented to perform several OSSEs in the North Atlantic (Halliwell et al., 2017a; Halliwell et al., 2017b; Halliwell et al., 2020).

2.2 Experimental set-up

First, the model was run to perform a hindcast of the year 2015. The initial conditions on January 1st, 2015, were taken from an unconstrained simulation running since January 1st, 2013, which was initialized from the Levitus climatology. In that 2015 reference experiment, called *Ref*, the model assimilated the following observations: along-track absolute dynamic topography (ADT) altimetry data from the Copernicus Marine Environment Monitoring Service (CMEMS, formerly AVISO), which is comparable to the model sea surface height (SSH), sea surface temperature (SST) from satellites (Multi-Channel Sea Surface Temperature, MCSST), drifters, buoys and ships of opportunity, and finally vertical profiles of temperature and/or salinity from Argo floats, ocean gliders, moorings, and expendable bathythermographs (XBTs).

A second experiment was then performed (namely *NoCarib*), which is identical to the *Ref* experiment except for the observations that were assimilated in the CS. In all other areas of the model domain, the observations that were assimilated are the same as in the *Ref* experiment, i.e. available along-track altimetry, SST, and vertical profiles of temperature and/or salinity. In the CS, the only observations that were assimilated were along-track climatological ADT altimetry data. The climatological ADT dataset was estimated by averaging, for each day of a calendar year, altimetry-derived
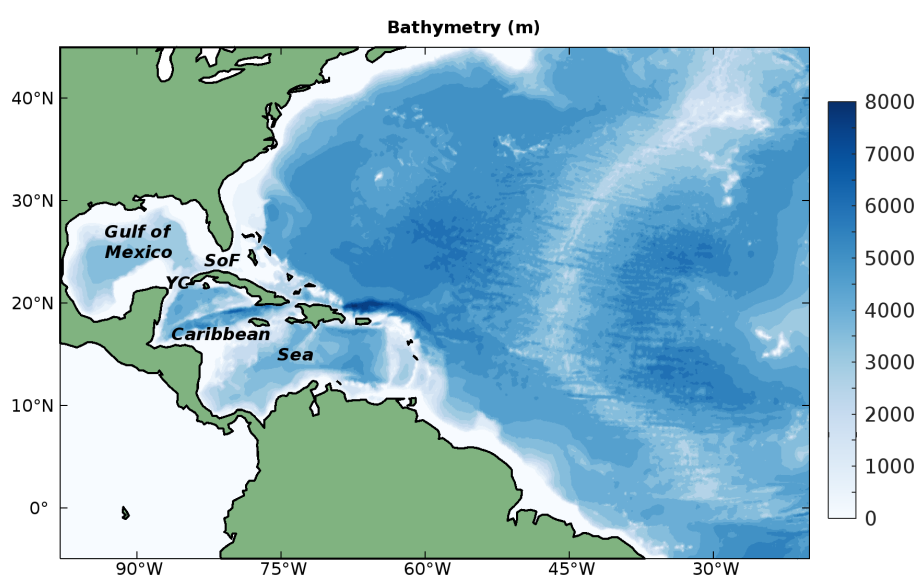

FIGURE 1
Model domain and bathymetry of the North Atlantic used in this study, with the main toponyms mentioned in the text (YC, Yucatan Channel; SoF, Straits of Florida).
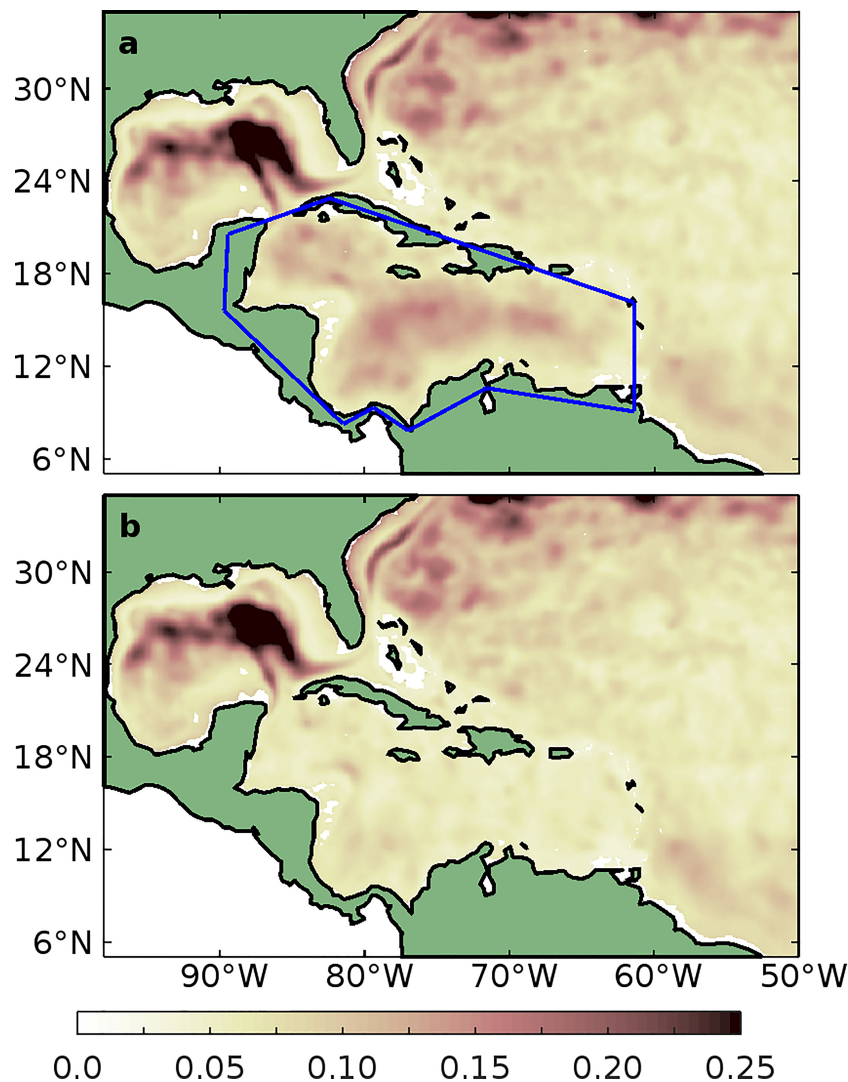
FIGURE 2
Temporal standard deviation in simulated Sea Surface Height (SSH, in meters) in the: **(A)** *Ref* and **(B)** *NoCarib* experiments during 2015. The blue box in **(A)** represents the extent of the Caribbean Sea in which the only assimilated observations in the *NoCarib* experiment were climatological SSH data. Please see text for details about the *Ref* and *NoCarib* experiments.

mapped ADT observed from 1993 to 2019. Climatological ADT values interpolated at the same day of the year and at the same locations as the actual along-track observations in 2015 were assimilated in the CS in the *NoCarib* experiment. Because the space and time variability in ADT (or SSH) is the signature of ocean mesoscale activity, replacing the actual altimetry observations with climatological values in the data that were assimilated leads to dampening the mesoscale activity in the model. This is visible on Figure 2, which shows the maps of the temporal standard deviation in model SSH estimated for the whole year in the *Ref* and *NoCarib* experiments. We clearly see that the standard deviation in SSH in the CS in the *NoCarib* experiment is close to 0, whereas in the *Ref* experiment it is much larger.

From these two data-assimilative experiments, we then ran a series of forecast simulations to investigate to what extent the presence or absence of eddy activity in the CS impact the LC predictions. For each experiment, we initiated 60-day forecasts

every 10 days, starting on day 30 of 2015 to allow for data assimilation to constrain the ocean state from the initial conditions. The last forecast was initiated on day 300 and ended on day 360 at the end of 2015. This corresponds to 28 forecast simulations per experiment, i.e. 56 forecast simulations in total (*Ref* and *NoCarib* together). We analyzed the daily model outputs from these model experiments and forecasts.

2.3 Analysis of model outputs

The first analysis of model outputs is based on the root-mean square error (RMSE) of the model SSH with respect to the daily mapped ADT altimetry observations from CMEMS. Since the observed mapped ADT field has a 0.25°spatial resolution, whereas the model grid has a resolution of 0.08°, the model SSH values were first smoothed and

interpolated onto the same grid as the mapped ADT observations, by averaging the model SSH over three grid intervals, i.e. 0.24°, which is very close to the resolution of the observed ADT, in both latitudinal and longitudinal directions around each ADT grid point. Then, since the mean SSH level in the HYCOM model is arbitrary, both the model SSH and the observed ADT fields need to be corrected before they can be compared. For the model SSH, this was done by removing, at each grid point, the temporal mean of the SSH from the realistic, data-assimilated *Ref* experiment over the whole of 2015. For the observations, this was done by removing, at each grid point, the temporal mean of the observed ADT over the whole of 2015. The RMSE in each ensemble of forecasts was estimated after completion of these steps.

The second analysis of model outputs is based on the evolution of the LC contour. We estimated the contour of the LC, for each daily output of each model forecast, by identifying the contour of the 17 cm anomaly in SSH with respect to the basin average, following the approach by Leben (2005). We did the same with the altimetry observations using the daily mapped ADT. We then used these daily LC contours to derive the time series of the northernmost extension of the LC, in the model forecasts and in the observations. Because an LCE detachment or separation is associated with the sudden retraction of the LC, any drop, from one day to the next, of the LC northern extension time series by 0.3 degree in latitude or more was considered to mark an LCE detachment. We verified visually that this threshold allows capturing actual LCE detachments by examining the time evolution of the SSH maps. For each of the 60-day forecast period, we estimated the day of the first eddy detachment or separation, if any, in the model forecasts as well as in the actual LC state observed by altimetry.

3 Results

3.1 Impact of the CS eddy field on the model SSH

We first compare the realism of the SSH field forecasted from both the *Ref* and *NoCarib* experiments in terms of RMSE. Figure 3 shows the

RMSE in forecasted SSH derived from the 28 forecast cycles initialized from the *Ref* experiment, for various forecast periods. As expected, we see the RMSE growing with time in the eastern GoM, associated with the LC. Because of its peculiar, highly non-linear behavior, and the difficulty in predicting it, the LC is associated with the largest RMSE in the region. Figure 4 shows the same RMSE but for the forecasts initialized from the *NoCarib* experiment. Similar to the forecasts from the *Ref* experiment, the RMSE is growing with time in the LC region within the GoM. One difference is that, in the initial forecast periods at 1 to 10 days and 11 to 20 days (Figures 3A, B, 4A, B), the RMSE of the forecasts initialized from the *NoCarib* experiment is slightly larger in the CS, with values reaching 0.15 to 0.2 m compared to values generally lower than 0.1 m in the *Ref* experiment. This is expected from the fact that the eddy field in the CS has been damped down in the *NoCarib* experiment. As a result, the forecasts are initialized with a non-realistic state and the errors in SSH are present from the start. For longer forecasts beyond 20 or 30 days, the RMSE levels appear to be comparable in the forecasts initialized from both experiments, with local differences that will now be discussed.

The differences between the RMSE achieved in the ensembles of forecasts initialized from both hindcast experiments are more visible on Figure 5. We clearly see, in the initial 1-10 day forecast period (Figure 5A), the large, positive RMSE difference (RMSE$_{NoCarib}$-RMSE$_{Ref}$) in the CS, which means that the forecasts initialized from the *Ref* experiment are closer to the observed ocean state than the forecasts initialized from the *NoCarib* experiment. As mentioned earlier, this RMSE difference stems from the perturbation strategy. The RMSE difference in the CS in that period is especially large in the eastern and western parts of the CS where the bathymetry is deep, which is where the signature of mesoscale eddies is expected to be large. During that same 1-10 day forecast period, the RMSE difference is small in the GoM, although the positive RMSE difference in the western part of the CS extends in the southeastern GoM, associated with water masses advected into the GoM. During the following forecast periods, at 11-20 and 21-30 days (Figures 5B, C), the RMSE difference tends to reduce in amplitude in the CS, as the memory of the different initial conditions constrained with data assimilation tends to
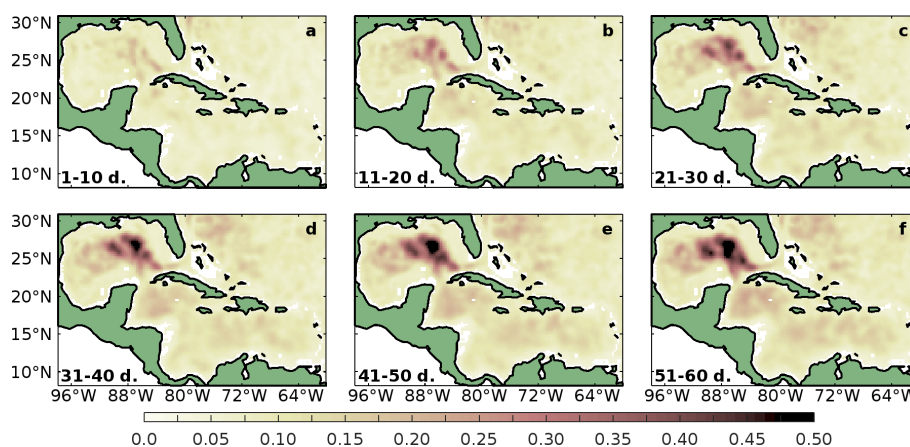

FIGURE 3
Root-mean square error in simulated Sea Surface Height (SSH, in meters) derived from the 28 forecast cycles initialized from the *Ref* experiment, averaged for the following forecast periods: **(A)** 1-10 days, **(B)** 11-20 days, **(C)** 21-30 days, **(D)** 31-40 days, **(E)** 41-50 days, and **(F)** 51-60 days.
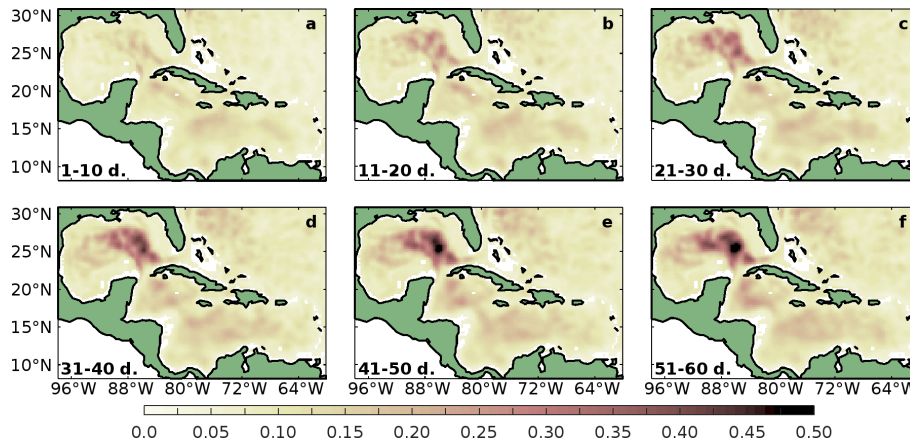
FIGURE 4
Same as Figure 3 but for the *NoCarib* experiment.

wane. On the other hand, during those periods the RMSE difference grows in the GoM, with positive differences in the southeastern GoM just north of the Yucatan Channel, whereas the RMSE difference is negative in other parts of the deep eastern GoM. This pattern is more pronounced in the 31-40 day forecast period (Figure 5D), during which the RMSE difference is positive in the eastern GoM between the Yucatan Channel and 25°N, whereas it is negative in other parts of the deep eastern and central GoM. In the CS, the RMSE difference remains positive in the eastern part of the basin, but it is more mixed in the western part of the basin south of the Yucatan Channel, with positive and negative patches. In the 41-50 day forecast period (Figure 5E), the RMSE difference in the GoM remains largely positive between the Yucatan Channel and 25°N, although with a lower amplitude than in the previous period. We also notice the presence of a patch of negative RMSE difference close to the Straits of Florida, which was present in the previous forecast period but moved southward between both periods. In the CS, the RMSE difference

remains positive in the eastern part of the basin, whereas, in the western part, a patch of negative RMSE difference is seen making its way into the Yucatan Channel toward the GoM. During the 51-60 day forecast period (Figure 5F), that patch merges with the patch of negative RMSE difference that was present in the southeastern GoM in the previous period, leading to a large portion of negative RMSE difference in the GoM just north of the Yucatan Channel. A patch of positive RMSE difference is still present in the eastern GoM around 25°N.

The forecast experiments show that, in the absence of a mesoscale eddy field in the CS in the initial conditions, the forecasted SSH tends to degrade with time in the southeastern GoM, with the largest signature in RMSE difference reached during the 31-40 day forecast period. However, in other parts of the eastern and central GoM, the forecasted SSH appears to have similar or even reduced errors with respect to the reference case, associated with negative RMSE differences. This suggests that the expected negative impact of dampening the CS mesoscale eddy field on the
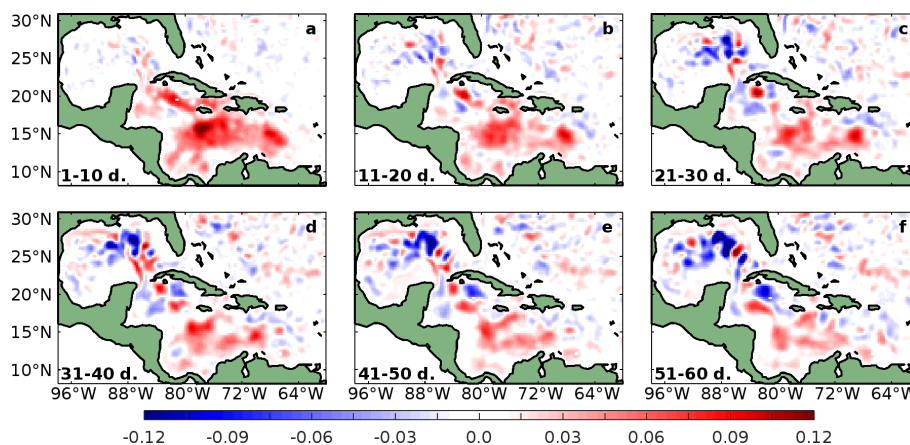

FIGURE 5
Differences in simulated SSH root-mean square errors (in meters) between the forecast cycles initialized from the *NoCarib* experiment and from the *Ref* experiment (RMSE$_{NoCarib}$-RMSE$_{Ref}$), averaged for the same forecast periods as in Figures 3, 4. Positive values indicate higher RMSE in the *NoCarib* experiment.
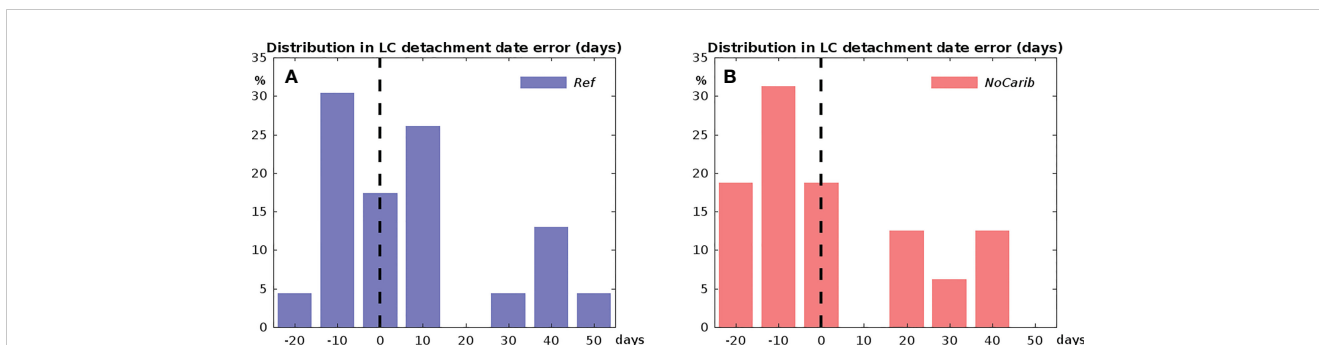
FIGURE 6
Distribution of the errors in the predicted date of the first LCE detachment during the 60-day forecast periods, normalized by the number of detachment cases, for: **(A)** the forecast cycles initialized from the *Ref* experiment, and **(B)** from the *NoCarib* experiment.

GoM SSH forecast is strongest, on average, at the region between the Yucatan Channel and 25°N, where the core of the LC is usually located.

3.2 Impact of the CS eddy field on LCE shedding

Although the RMSE in SSH in the eastern GoM is a relevant metric to analyze the ocean dynamical processes associated with the LC system, it is not the most adapted to analyze the LCE shedding events, which is the focus of this study. We thus now consider the impact of dampening the CS eddy field on the forecast of the LCE shedding events, using the day of the first LCE detachment, as described in Section 2.3, in each model forecast period.

Figure 6 presents the normalized distribution of the errors in the day of the first detachment, estimated for each forecast period for all forecasts initialized by both the *Ref* and the *NoCarib* experiments. The error was estimated by comparing the day of the first LCE detachment in a given forecast with the day of an actual LCE detachment identified using altimetry in that same forecast period. A negative error indicates that the model forecasted an LCE detachment after it was actually observed, whereas a positive error indicates that the model forecasted an LCE detachment before it was actually observed. The distributions were normalized by the total number of LCE detachments taking place in each ensemble, which differ from the total number of observed LCE detachments, as will be examined later. Figure 6A shows that the errors in the LCE detachment date in the forecasts initialized from the *Ref*

experiment range from -20 to 50 days, with 74% of the forecasted LC detachments associated with errors between -15 and 15 days. On the other hand, the errors in the LCE detachment date in the forecasts initialized from the *NoCarib* experiment are less often close to 0 (Figure 6B), with 50% of the forecasted LC detachments with errors between -15 and 15 days. Thus, the LCE detachment dates in the forecasts initialized with realistic ocean conditions in the CS (*Ref* forecasts) are more often close to the observed detachment dates than in the absence of the CS mesoscale eddy field (*NoCarib* forecasts).

In addition to the errors in the LCE detachment date, we examined the cases in which a detachment was incorrectly predicted to take place or not. These errors include the false positive LCE detachment predictions, i.e. cases for which an LCE detachment was predicted by the model forecasts within the 60-day forecast period but was not actually observed, and the false negative LCE detachment predictions, i.e. cases for which an LCE detachment was not predicted within the 60-day forecast period but was actually observed. Table 1 shows that the level of false positive cases is identical in both ensembles of forecast (3 out of 28 cycles), but the level of false negative cases is much larger in the forecasts initialized from the *NoCarib* experiment (9) than in the forecasts initialized from the *Ref* experiment (2). This means that, in the absence of the CS eddy field in the initial conditions, the model tends to underestimate the number of LCE detachment events within the 60 days of the forecast period.

Considering both the normalized distribution of the errors in the LCE detachment dates and the level of false negative LCE detachment predictions, 68% of the actual LCE detachments were predicted with an error of 15 days or less in the forecasts initialized

TABLE 1 False positive and false negative cases in the prediction of the date of the first LCE detachment during the 28 60-day forecast periods, for the forecast cycles initialized from the *Ref* experiment and from the *NoCarib* experiment.

Initial conditions for the forecasts	*Ref*	*NoCarib*
False positive (LCE detachment predicted but not observed)	3	3
False negative (LCE detachment not predicted but observed)	2	**9**

bold character stress that it is remarkable.

from the *Ref* experiment, but only 32% in the forecasts initialized from the *NoCarib* experiment.

4 Discussion and conclusions

In this study, we performed two data-assimilative experiments in the North Atlantic using the HYCOM model at 1/12° resolution, one assimilating all available observations (*Ref*) and one assimilating all available observations except in the Caribbean Sea (CS), where only climatological altimetry data were assimilated, leading to the dampening of the eddy activity there (*NoCarib*). These two experiments were used to initialize 28 forecasts of 60-day length for each case, totaling 56 forecast experiments. In terms of Sea Surface Height (SSH), the forecasts initialized with the *Ref* experiment had, on average, lower errors than the forecasts initialized with the *NoCarib* experiment in the southeastern part of the Gulf of Mexico (GoM) north of the Yucatan Channel, with a peak during the 31-40 day forecast period. In addition, in the absence of mesoscale eddy activity in the CS in the initial conditions, the errors in the predicted date of a Loop Current (LC) Eddy detachment tend to be larger, whereas these errors are more centered around zero in the forecasts initialized with the realistic, *Ref* experiment. More importantly, the rate of false predictions of an absence of a detachment, whereas a detachment was actually observed, is much larger in the forecasts initialized with dampened mesoscale eddy activity in the CS. As a result, 68% of actual Loop Current Eddy (LCE) detachments were predicted with an error of 15 days or less in the forecasts initialized with the *Ref* experiment, but only 32% in the forecasts initialized from the *NoCarib* experiment.

Our results show the importance of the eddy field in the CS for the prediction of the LC system. In terms of SSH, the absence of the CS eddy field leads to degrading the forecasts in the southeastern GoM, which was expected, although this is not necessarily the case in large portions of the eastern and central GoM. This result is associated with outlier members of the ensemble of forecasts initialized with the *Ref* experiment, in which the LC retracts after shedding an LCE, whereas in the observations the LCE either detaches much later or the LC reattaches after the LCE detachment. This led to large discrepancies in SSH in the model forecasts in the area where the extended LC usually evolves, i.e. north of 25°N in the eastern and central GoM. In the other ensemble initialized with the *NoCarib* experiment, in the same cases the LC tends to remain extended, consistent with the high rate of false negative LCE detachment predictions derived from that ensemble. For these cases, the discrepancies in SSH in the model forecasts are significantly smaller than in the ensemble initialized with the *Ref* experiment, leading to the patches of negative RMSE difference seen on Figure 5.

The smaller error in the LCE detachment date for the forecasts initialized with the *Ref* experiment rather than the *NoCarib* experiment shows that the eddy field is important for the timing of the LCE detachment. This result is in agreement with Androulidakis et al. (2021), who showed that the passage of anticyclonic Caribbean Eddies from the CS to the GoM tend to precede a retraction of the LC in the GoM, and also with Athié et al.

(2012), who found that cyclonic perturbations or eddies present in the CS and entering the GoM are often involved in the LCE shedding process. Moreover, the large number of false negative cases in the LCE detachment forecasts initialized with the *NoCarib* experiment shows that the eddy activity in the CS is crucial for the LCE detachment process to even happen, not to mention with the correct timing. These false negative forecasts correspond to cases in which no LCE detachment was predicted within the 60-day forecast period, whereas an LCE detachment actually took place. This result is consistent with Oey et al. (2003), who found that the presence of anticyclonic eddies in the Caribbean Sea tended to delay the frequency of LCE shedding by over 5 months, i.e. much longer than the 2-month period of the forecast experiments run here. It is also consistent with Garcia-Jove et al. (2016), who found that suppressing eddies in the CS in their model reduces the number of LCE separations and increases the mean LCE separation interval by about 2 months.

Our study is thus consistent with the few previous studies that discuss the impact of the eddy field in the CS on the GoM dynamics and the LCE shedding process. However, it is the first study, to our knowledge, that addresses this topic from the perspective of ocean model forecasts, and our results clearly show that the eddy field in the CS is essential to the correct prediction of the LCE shedding events and their timing. This result is important for near-real time and operational prediction systems, especially the regional systems focusing on forecasting the GoM and the LC evolution. Such systems have to include a large portion of the CS, constrained with data assimilation, or pay particular attention to accurate boundary conditions from the CS upstream of the GoM, if the LC evolution is to be realistically predicted. This result is of particular importance for applications in the GoM that depend on the correct prediction of the LC state at a range of a few weeks, especially the ones related to the oil industry. Such applications justified the current effort, from the National Academy of Sciences, Engineering, and Medicine to implement its UGOS initiative. Future work along the lines presented here could include a comparable study with a higher resolution model, which would allow examining the impact of the smaller mesoscale and sub-mesoscale processes in the CS on the LC and the GoM dynamics, which is still little known.

Data availability statement

The raw data supporting the conclusions of this article will be made available by the authors, without undue reservation.

Author contributions

MLH led the design of the study, performed some of the numerical experiments, and led the analysis of the results. VK helped in the design of the study and in the analysis of the results. YA and NN helped in the analysis of the results. HK performed some of the numerical experiments. ML led the writing of the manuscript, with the help of all co-authors. All authors contributed to the article and approved the submitted version.

Conflict of interest

The authors declare that the research was conducted in the absence of any commercial or financial relationships that could be construed as a potential conflict of interest.

The handling editor SM declared a shared consortium with the author MLH at the time of the review.

Publisher's note

All claims expressed in this article are solely those of the authors and do not necessarily represent those of their affiliated organizations, or those of the publisher, the editors and the reviewers. Any product that may be evaluated in this article, or claim that may be made by its manufacturer, is not guaranteed or endorsed by the publisher.

References

Androulidakis, Y., Kourafalou, V., Olascoaga, M. J., Beron-Vera, F. J., Le Hénaff, M., Kang, H., et al. (2021). Impact of Caribbean anticyclones on loop current variability. *Ocean Dyn.* 71 (9), 935–956. doi: 10.1007/s10236-021-01474-9

Athié, G., Candela, J., Ochoa, J., and Sheinbaum, J. (2012). Impact of Caribbean cyclones on the detachment of loop current anticyclones. *J. Geophys. Res.* 117 (C3). doi: 10.1029/2011JC007090

Bleck, R. (2002). An oceanic general circulation framed in hybrid isopycnic-Cartesian coordinates. *Ocean Model.* 4, 55–88. doi: 10.1016/S1463-5003(01)00012-9

Candela, J., Ochoa, J., Sheinbaum, J., Lopez, M., Perez-Brunius, P., Tenreiro, M., et al. (2019). The flow through the gulf of Mexico. *J. Phys. Oceanogr.* 49 (6), 1381–1401. doi: 10.1175/JPO-D-18-0189.1

Candela, J., Sheinbaum, J., Ochoa, J. L., Badan, A., and Leben, R. (2002). The potential vorticity flux through the Yucatan channel and the loop current in the gulf of Mexico. *Geophys. Res. Lett.* 29 (22), 2059. doi: 10.1029/2002GL015587

Chang, Y.-L., and Oey, L.-Y. (2012). Why does the loop current tend to shed more eddies in summer and winter? *J. Geophys. Res.* 39, L05605. doi: 10.1029/2011GL050773

Chassignet, E. P., Smith, L. T., Halliwell, G. R.Jr., and Bleck, R. (2003). North Atlantic simulation with the HYbrid coordinate ocean model (HYCOM): impact of the vertical coordinate choice, reference density, and thermobaricity. *J. Phys. Oceanogr.* 33, 2504–2526. doi: 10.1175/1520-0485(2003)033<2504:NASWTH>2.0.CO;2

Chérubin, L. M., Morel, Y., and Chassignet, E. P. (2006). Loop current ring shedding: The formation of cyclones and the effect of topography. *J. Phys. Oceanogr.* 36 (4), 569–591. doi: 10.1175/JPO2871.1

Donohue, K. A., Watts, D. R., Hamilton, P., Leben, R., and Kennelly, M. (2016a). Loop current eddy formation and baroclinic instability. *Dyn. Atmos. Oceans* 76, 195–216. doi: 10.1016/j.dynatmoce.2016.01.004

Donohue, K. A., Watts, D. R., Hamilton, P., Leben, R., Kennelly, M., and Lugo-Fernández, A. (2016b). Gulf of Mexico loop current path variability. *Dyn. Atmos. Oceans* 76, 174–194. doi: 10.1016/j.dynatmoce.2015.12.003

Dukhovskoy, D. S., Leben, R. R., Chassignet, E. P., Hall, C. A., Morey, S. L., and Nedbor-Gross, R. (2015). Characterization of the uncertainty of loop current metrics using a multidecadal numerical simulation and altimeter observations. *Deep Sea Res. Part I Oceanogr. Res. Pap.* 100, 140–158. doi: 10.1016/j.dsr.2015.01.005

Garcia-Jove, M., Sheinbaum, J., and Jouanno, J. (2016). Sensitivity of loop current metrics and eddy detachments to different model configurations: The impact of topography and Caribbean perturbations. *Atmosfera* 29, 235–265. doi: 10.20937/ATM.2016.29.03.05

Halliwell, G. R. (2004). Evaluation of vertical coordinate and vertical mixing algorithms in the hybrid-coordinate ocean model (HYCOM). *Ocean Model.* 7, 285–322. doi: 10.1016/j.ocemod.2003.10.002

Halliwell, G. R., Goni, G. J., Mehari, M. F., Kourafalou, V. H., Baringer, M., and Atlas, R. (2020). OSSE assessment of underwater glider arrays to improve ocean model

initialization for tropical cyclone prediction. *J. Atmos. Ocean Technol.* 37 (3), 467–487. doi: 10.1175/JTECH-D-18-0195.1

Halliwell, G. R., Mehari, M., Le Hénaff, M., Kourafalou, V. H., Androulidakis, Y. S., Kang, H.-S., et al. (2017a). North Atlantic ocean OSSE system: evaluation of operational ocean observing system components and supplemental seasonal observations for potentially improving tropical cyclone prediction in coupled systems. *J. Oper. Oceanogr.* 10 (2), 154–175. doi: 10.1080/1755876X.2017.1322770

Halliwell, G. R. Jr., Mehari, M., Shay, L. K., Kourafalou, V. H., Kang, H., Kim, H.-S., et al. (2017b). OSSE quantitative assessment of rapid-response prestorm ocean surveys to improve coupled tropical cyclone prediction. *J. Geophys. Res.* 122 (7), 5729–5748. doi: 10.1002/2017JC012760

Halliwell, G. R., Srinivasan, A., Kourafalou, V. H., Yang H, H., Willey, D., Le Hénaff, M., et al. (2014). Rigorous evaluation of a fraternal twin ocean OSSE system in the open gulf of Mexico. *J. Atmos. Ocean Technol.* 31, 105–130. doi: 10.1175/JTECH-D-13-00011.1

Hiron, L., Jaimes de la Cruz, B., and Shay, L. K. (2020). Evidence of loop current frontal eddy intensification through local linear and nonlinear interactions with the loop current. *J. Geophys. Res.* 125 (4), p.e2019JC015533. doi: 10.1029/2019JC015533

Hurlburt, H. E., and Thompson, J. D. (1980). A numerical study of loop current intrusions and eddy shedding. *J. Phys. Oceanogr.* 10, 1611–1651. doi: 10.1175/1520-0485(1980)010<1611:ANSOLC>2.0.CO;2

Hurlburt, H. E., and Thompson, J. D. (1982). "The dynamics of the loop current and shed eddies in a numerical model of the gulf of Mexico," in *Hydrodynamics of semi-enclosed seas*. Ed. J. C. J. Nihoul (Liege: Elsevier Oceanography Series, Elsevier) 34, 243–297. doi: 10.1016/S0422-9894(08)71247-9

Kaiser, M. J., and Pulsipher, A. G. (2007). The impact of weather and ocean forecasting on hydrocarbon production and pollution management in the gulf of Mexico. *Energy Policy* 35 (2), 966–983. doi: 10.1016/j.enpol.2006.01.026

Lara-Hernández, J. A., Zavala-Hidalgo, J., Sanvicente-Añorve, L., and Briones-Fourzán, P. (2019). Connectivity and larval dispersal pathways of panulirus argus in the gulf of Mexico: A numerical study. *J. Sea Res.* 155, 101814. doi: 10.1016/j.seares.2019.101814

Leben, R. R. (2005). *Altimeter-derived loop current metrics, in circulation in the gulf of Mexico: Observations and models* Vol. vol. 161. Eds. W. Sturges and A. Lugo-Fernandez (Washington, D. C: AGU), 181–201.

Le Hénaff, M., Kourafalou, V. H., Dussurget, R., and Lumpkin, R. (2014). Cyclonic activity in the eastern gulf of Mexico: characterization from alongtrack altimetry and *in situ* drifter trajectories. *Prog. Oceanogr.* 120, 120–138. doi: 10.1016/j.pocean.2013.08.002

Le Hénaff, M., Kourafalou, V. H., Morel, Y., and Srinivasan, A. (2012b). Simulating the dynamics and intensification of cyclonic loop current frontal eddies in the gulf of Mexico. *J. Geophys. Res.* 117 (C2), C02034. doi: 10.1029/2011JC007279

Le Hénaff, M., Kourafalou, V. H., Paris, C. B., Helgers, J., Aman, Z. M., Hogan, P. J., et al. (2012a). Surface evolution of the deepwater horizon oil spill patch: combined effects of circulation and wind-induced drift. *Environ. Sci. Technol.* 46, 7267–7273. doi: 10.1021/es301570w

Lipphardt, B., Poje, A. C., Kirwan, A., Kantha, L., and Zweng, M. (2008). Death of three loop current rings. *J. Mar. Res.* 66 (1), 25–60. doi: 10.1357/0022240 08784815748

Lugo-Fernández, A. (2018). Modeling the intrusion of the loop current into the gulf of Mexico. *Dyn. Atmos. Oceans* 84, 46–54. doi: 10.1016/j.dynatmoce.2018.10.003

Oey, L.-Y. (2004). Vorticity flux through the Yucatan channel and loop current variability in the gulf of Mexico. *J. Geophys. Res.* 109, C10004. doi: 10.1029/2004JC002400

Oey, L.-Y., Lee, H.-C., and Schmitz, W. J.Jr. (2003). Effects of winds and Caribbean eddies on the frequency of loop current eddy shedding: A numerical model study. *J. Geophys. Res.* 108 (C10), 3324. doi: 10.1029/2002JC001698

Pichevin, T., and Nof, D. (1997). The momentum imbalance paradox. *Tellus A* 49 (2), 298–319. doi: 10.3402/tellusa.v49i2.14484

Schmitz, W. J. (2005). "Cyclones and westward propagation in the shedding of anticyclonic rings from the loop current," in *Circulation in the gulf of Mexico: Observations and models*, vol. vol. 161 . Ed. W. Sturges and A. Lugo-Fernandez (Washington, D. C: AGU), 241–261.

Sheinbaum, J., Athié, G., Candela, J., Ochoa, J., and Romero-Arteaga, A. (2016). Structure and variability of the Yucatan and loop currents along the slope and shelf break of the Yucatan channel and campeche bank. *Dyn. Atmos. Oceans* 76, 217–239. doi: 10.1016/j.dynatmoce.2016.08.001

Vidal, V. M., Vidal, F. V., and Pérez-Molero, J. M. (1992). Collision of a loop current anticyclonic ring against the continental shelf slope of the western gulf of Mexico. *J. Geophys. Res.* 97 (C2), 2155–2172. doi: 10.1029/91JC00486

Vukovich, F. M. (2007). Climatology of ocean features in the gulf of Mexico using satellite remote sensing data. *J. Phys. Oceanogr.* 37 (3), 689–707. doi: 10.1175/JPO2989.1

Zavala-Hidalgo, J., Morey, S. L., and O'Brien, J. J. (2003). Cyclonic eddies northeast of the campeche bank from altimetry data. *J. Phys. Oceanogr.* 33, 623–629. doi: 10.1175/1520-0485(2003)033<0623:CENOTC>2.0.CO;2